RADIATION DRIVEN WINDS OF HOT STARS: THEORY OF O-STAR ATMOSPHERES AS A SPECTROSCOPIC TOOL

A.W.A. PAULDRACH, A. FELDMEIER, J. PULS and R.P. KUDRITZKI*
Universitatssternwarte Munchen, D-81679 Munchen, Scheinerstrae 1, Federal Republik of Germany

Abstract. The status of the continuing effort to construct radiation driven wind models for O-Stars atmospheres is reviewed. Emphasis is given to several problems relating to the fomation of UV line spectra the use of accurate atomic data, the inclusion of EUV radiation by shock heated matter, the simulation of photospheric line blocking.

A new tool for O-star diagnostics is presented. This is based on the use of wind models to calculate synthetic high resolution spectra covering the observable UV region. A comparison with observed spectra then gives physical constraints on the properties of stellar winds and stellar parameters, additionally abundances can be determined.

The astrophysical potential of this method is demonstrated by an application to two Of-stars, the galactic O4f-star ζ-Puppis and the LMC O3f-star Melnick 42. With regard to effective temperatures and gravities, the results from the application of classical methods to the analysis of photospheric lines are only partially verified. Explanations for the shortcomings of classical NLTE methods are discussed.

Key words: stars: atmospheres, early-type, mass-loss, X-rays, fundamental parameters, element abundances

1. Introduction

Although the ultraviolet spectra of O-stars with their hundreds of spectral lines provide a wealth of astrophysically important information about plasma conditions, stellar parameters and abundances, the quantitative analysis of UV O-star spectra concentrates on the few strong stellar wind lines (in particular the resonance lines of CIV, NV, OVI and SiIV). However, numerous other strong wind contaminated lines, especially of the iron group elements (see Fig. 1), are not taken into account. This is dangerous since, due to the usual uncertainty of stellar parameters and abundances (see below) and the complexity of the theory of O-star atmospheres, the uniqueness of an atmospheric model can not be guaranteed by fitting only a few wind lines. This means that an atmospheric model, and the stellar parameters derived from that, can be regarded as correct only if the consistently calculated synthetic high resolution spectrum covering the full observable UV spectral range fits the observed spectrum.

The theoretical tools which are required for this objective are still in an explorative stage. There are two reasons for that:

First, the simplifying assumption of LTE fails completely in O-star atmospheres because of the intense radiation field and, thus, a NLTE treatment of all

* RPK affiliated to Max-Planck-Inst. fur Astrophys., Karl-Schwarzschild-Str. 1, D-85748 Garching bei Munchen, Federal Republik of Germany

Space Science Reviews **66**: 105–125, 1994.

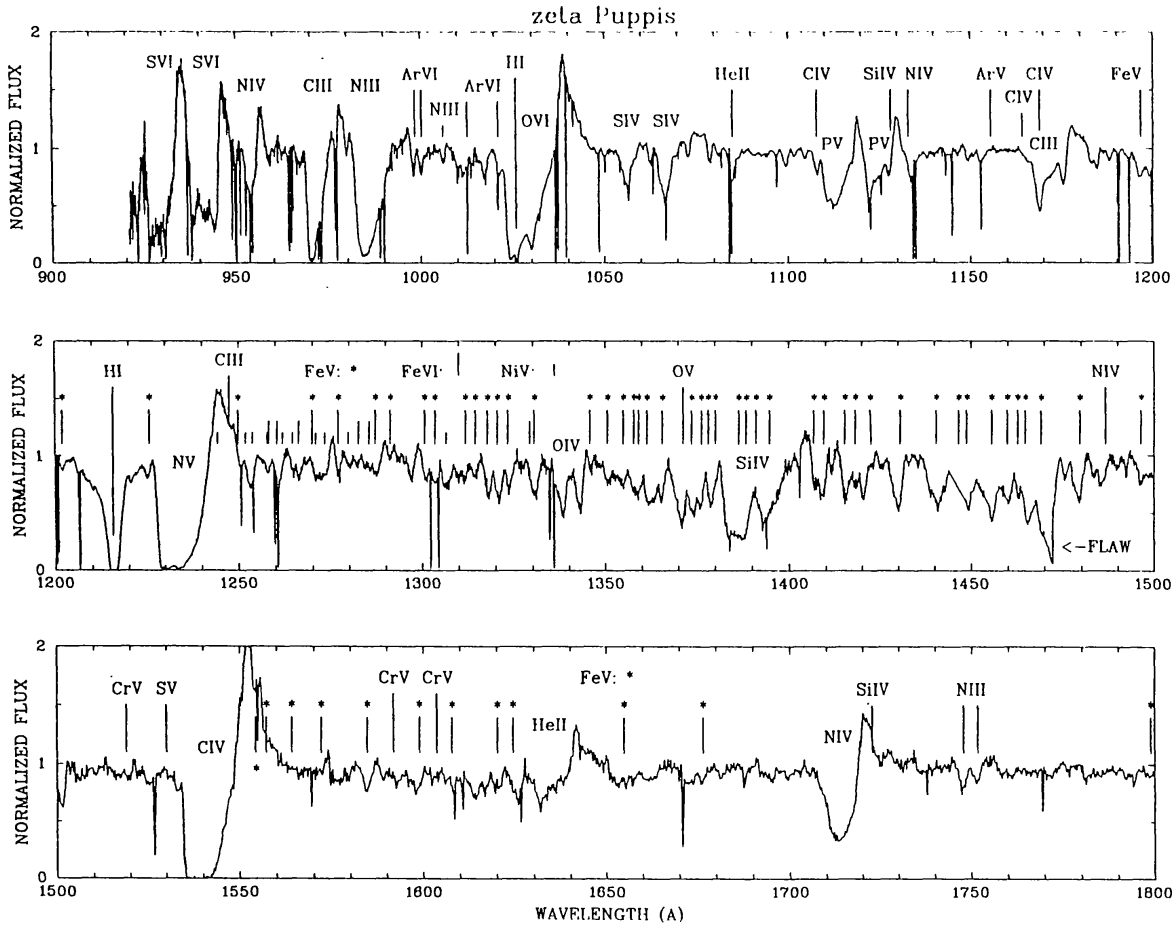

Fig. 1. Observed Copernicus (900-1500A, Morton and Underhill (1977)) and IUE (1500-1800A, Walborn et al. (1985)) high resolution UV spectrum. A large number of strong and weak winds lines are identified and marked. Note the numerous FeV lines between 1250 and 1500A.

ions including the iron group elements is needed. As has become evident during the past decade, such NLTE calculations, if they are to be used for a quantitative comparison with observations, require very detailed and sophisticated model atoms with a large number of energy levels and transitions and with sufficiently accurate atomic data. Second, the UV line spectrum is strongly affected by the presence of stellar winds. This is true not only for the few strong resonance lines that exhibit P-Cygni profiles but also for the many weak absorption lines observed. In consequence, a hydrodynamic model atmosphere treatment that includes the effects of stellar winds is needed for theoretical spectrum synthesis calculations in the ultraviolet.

Usually the basic parameters of O-stars, consisting of effective temperature and gravity, are determined by an analysis of photospherical H and He lines (cf. Kudritzki and Hummer, 1990). These parameters enter in the hydrodynamical calculations as a starting point. Hence, it is important to note that these lines are affected by stellar winds as well (cf. Gabler et al. 1989). This effect can be clearly seen in Fig. 2 where the observed H_γ line profile of the two Of-stars (ζ-Puppis

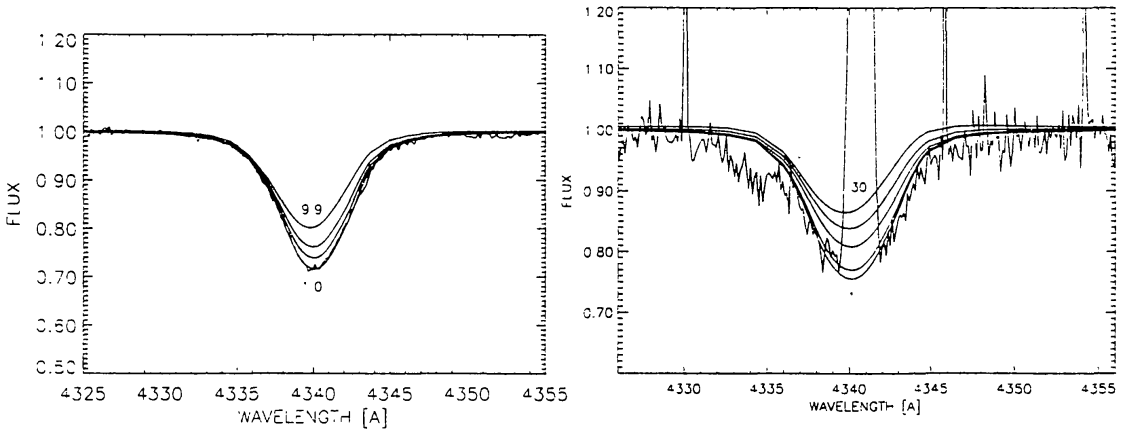

Fig. 2. Observed and calculated Hγ profiles of ζ Puppis (Left - a sequence of $\dot{M} = 1.0, 3.2, 5.5, 9.9 \cdot 10^{-6} M_{\odot}/yr$ was adopted for the various models) and Melnick 42 (right - $\dot{M} = 1.0, 3.3, 10., 20., 30. \cdot 10^{-6} M_{\odot}/yr$ was adopted). From Sellmaier et al. (1993).

and Melnick 42) are compared to a sequence of "unified models" (photospherical NLTE models which include spherical extension and stellar winds) with different mass loss rates. The effect of wind contamination fills up the absorption profile with increasing mass loss rate. To fit the observed profile a higher value for the surface gravity is required (cf. Sellmaier et al. 1993). However, as is shown in Fig. 2, the influence of wind contamination can just be quantified if the hydrodynamical structure and hence the mass loss rate is known; but this requires a knowledge of the stellar parameters in advance. Although the procedure is straightforward in the case the value for the mass loss rate is not too high (for ζ-Puppis with $\dot{M} = 3 - 5\ 10^{-6} M_{\odot}/yr$ an enhancement of 0.1-0.15 dex is required for the surface gravity, Sellmaier et al. , 1993), almost nothing can be predicted in cases where the value for the mass loss rate is highly uncertain. In sect. 3 it will be shown that Melnick 42 belongs to this class of objects where only a lower limit for the basic parameters can be obtained from a photospheric analysis. We also review in that section a recently developed step towards fully quantitative UV-spectroscopy of O-stars based on NLTE radiation driven wind models, and we point out that this kind of spectroscopy can fill the diagnostic gap shown to exist for O-stars like Melnick 42, i.e. objects with high and uncertain mass loss rates. For this purpose the concept and the status of the computational method is summarized in sect. 2.

2. The Theory of Radiation Driven Winds

The basis of our model calculations is the concept of homogeneous, stationary and spherically symmetric radiation driven winds (where the driving mechanism is the line scattering of the photospheric UV radiation field by metal ions in the expanding and hence Doppler-shifted atmosphere) that describes correctly the

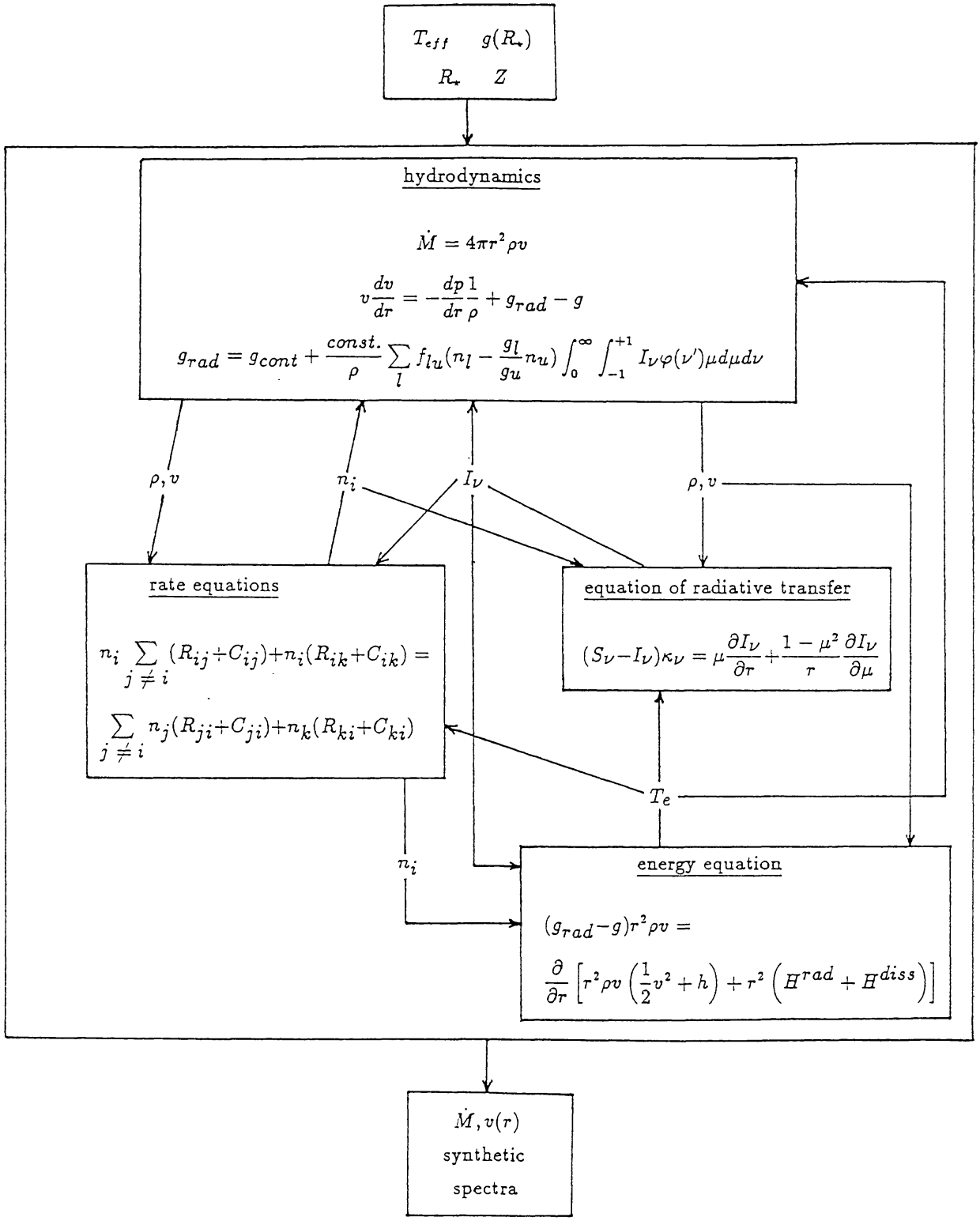

Fig. 3. Schematic sketch of the non-linear system of integro-differential equations that form the basis of stationary radiation driven wind theory (see text).

time average mean of most spectral features in the UV (see below). This paper is intended to summarize the status of radiation driven wind models and not to give a comprehensive review of the wind theory of hot stars. Before we start to describe the theory in its present form it should not be forgotten that the basic

ideas of the theory and the first attempt at its solution was the fundamental work of Lucy and Solomon (1970) and that the pioneering step in the formulation of the theory in a self-consistent manner was performed by Castor, Abbott and Klein (1975) and Abbott (1982). Although their approaches where only qualitative due to many simplifications, the theory was only further developed owing to their promising results.

The concept and the status of this development are sketched in Fig. 3. (essential steps of this building have been described and performed by Pauldrach, Puls and Kudritzki (1986, Paper I), Pauldrach (1987, Paper III), Puls (1987, Paper IV), Pauldrach and Herrero (1988), Pauldrach et al. (1990, Paper VII), Pauldrach et al. (1990, Paper IX) and Pauldrach et al. (1993, Paper XII).

To calculate a wind model, the stellar parameters T_{eff} (effective temperature), log g (logarithm of photospheric gravitational acceleration), R_* (photospheric radius defined at a pre-specified Thomson optical depth) and Z (abundances) have to be specified. Then the stationary hydrodynamic equations are solved in spherical symmetry (r is the radial coordinate, ϱ the mass density, v the velocity, p the gas pressure and $\dot{M}$ the rate of mass-loss). The crucial term is the radiative acceleration g_{rad} that has contributions from continuous absorption and scattering (g_{cont} - Thomson scattering, bound-free and free-free absorption of all elements considered (see below) are taken into account) and the line absorption. The calculation of the line acceleration is performed by summing the contributions of more than 200000 lines (see Paper XII). For each line the oscillator strengths f_{lu}, the statistical weights g_l, g_u and the occupation numbers n_l, n_u of the lower and upper level enter together with the frequency and angle integral over the specific intensity I_ν and the line broadening function φ_ν accounting for the Doppler effect.

The occupation numbers are determined by the *rate equations* containing collisional (C_{ij}) and radiative (R_{ij}) transition rates. It is important to note that the hydrodynamical equations are coupled directly with the rate equations. The velocity field enters into the radiative rates while the density is important for the collisional rates and the equation of particle conservation. On the other hand, the occupation numbers are crucial for the hydrodynamics since the radiative line acceleration dominates the equation of motion.

In addition, the radiation field determined by the *equation of transfer* is coupled with the hydrodynamics (radiative line acceleration) and the rate equations (radiative rates).

The temperature is, in principle, determined by the energy equation, which depends on h, the free enthalpy, H^{rad} the radiative flux and H^{diss} the energy flux generated by dissipative processes. Since we showed in Paper XII that the emergent spectrum is insensitive to the wind temperature structure used in our code we assumed a temperature structure on the basis of radiative equilibrium where bound-bound and bound-free opacities have been treated in NLTE and the effects of adiabatic cooling have been included (cf. Gabler, 1992).

The iterative solution of the total system of equations then yields the hydrodynamic structure of the wind – including *mass-loss rate* and *terminal velocity* (v_∞) together with synthetic spectra (see Puls and Pauldrach (1990) and Paper XII) that can be compared with observations.

Since our treatment of O-star atmospheric models was recently described comprehensively in Paper XII, we mention only the crucial points which either will have important consequences or still imply some uncertainties for our model calculations.

2.1. Atomic models

For detailed NLTE spectrum snthesis calculations, accurate atomic data are required. We are presently replacing the simplified atomic models (cf. Paper III, Paper IX) of the 149 ionization stages of 26 elements considered. This has already been done for the most important ionization stages, where more energy levels (comprising a total of 5000) and transitions (comprising 25000 bound-bound transitions and 20000 individual transition probabilities of low-temperature dielectronic recombination) were included for the following ions: H I; He I, II; C III, IV, V; N III, IV, V, VI; O IV, V, VI; Si IV; P V, VI; S VII; Ar VI, VII, VIII; Fe IV, V, VI ,VII, VIII; Ni V, VI, VII, VIII. To implement these improvements we utilised and modified the program SUPERSTRUCTURE (Eissner et al. 1974, Nussbaumer and Storey 1978), which uses the configuration interaction approximation to determine wavefunctions and radiative data.

2.2. Radiative rates and radiation transfer

i) For the calculation of the radiative bound-bound transition probabilities R_{ij} the Sobolev-approximation is used in the entire atmosphere. As this might be a poor approximation in the subsonic region of the atmospheric layers where the continuum is formed, we presently implement improvements such as the Sobolev plus continuum method (Hummer and Rybicki, 1985; Puls and Hummer, 1988) or the comoving frame method (for applications in stellar wind dynamics, see Puls, 1987).

ii) Low-temperature dielectronic recombination is included in the approximation described by Mihalas and Hummer (1973).

iii) The spherical transfer equation which yields the continous radiation field at up to 900 frequency points at every depth point including the deepest layers where the radiation is thermalized and the diffusion approximation is applicable is correctly solved, but without line opacities. Hence, the effects of photospheric EUV line blocking - due to metal ions in the spectral region between 228A and 911A - on the ionization and excitation of levels are treated separately in a realistic but still approximate way (see section 3.).

iv) The emission from shocks arising from the non-stationary, unstable behaviour of radiation driven winds (cf. Lamers et al., 1982; Prinja and Howarth, 1986; Henrichs, 1986; Ebbets, 1982; Bieging et al., 1989) is additionally taken

into account in the rate equations and the radiative transfer. This source was incorporated in a preliminary way on the basis of an approximate calculation of the shock emission coefficient (see section 3.).

v) Using the cross-sections from Deltabuit and Cox (1972) the K-shell absorption was included for C, N, O, Ne, Mg, Si and S in the radiative transfer and Auger- ionization was taken into account in the rate equations (see Hunsinger and Pauldrach, 1994).

This present approach to the theory of O-star atmospheres is obviously not free from approximations. However, a detailed comparison with the observations can demonstrate its reliability.

3. Wind models: towards detailed UV line diagnostics of O-stars

The objectives of a detailed comparison are twofold. The primary aim in a first step concerns the investigation of wind physics in order to find physical constraints on the properties of stellar winds and in order to prove our method. If this step has been successfully completed we will try to determine stellar parameters and abundances by means of UV spectral synthesis. Concerning the first point the galactic O4f-star ζ-Puppis has been chosen, since excellent high resolution UV spectra including the important EUV spectral range have been obtained with the Copernicus satellite (see Fig. 1), and accurate flux measurements at radio-, IR- and X-ray wavelengths are available. The method is then applied to the O3 If*/WN6 – A (Walborn et al., 1993) star Melnick 42-observed with HST by Heap et al. (1991)-in the 30 Dorados complex of the LMC, which is a suitable candidate due to the uncertainty of its stellar parameters (see section 1- for a more detailed discussion see Paper XII) and its extreme nature.

It is a very interesting result that hydrostatic NLTE analyses yielded almost identical basic parameters for ζ-Puppis (T_{eff} = 42000K, log g = 3.5 - Kudritzki et al. (1983), Bohannan et al. (1986), Voels et al. (1989) - $R/R_\odot$ = 19) and MK 42 (T_{eff} = 42500K, logg = 3.5 - Heap et al. (1991) - $R/R_\odot$ = 28), whereas the UV spectra of these objects look rather different. This points to the necessity of a quantitative treatment of the full UV-spectrum. *The strategy of our procedure is as follows:*

i) Starting from an adopted value of T_{eff} and an estimate of R_* and abundances (Z) the observed value of the terminal velocity is fitted by a sequence of models with varying log g. This gives $\dot{M}$ and the *surface gravity* which can be compared to the value obtained from the "unified models".

ii) Then, a model grid is calculated and the corresponding synthetic UV high resolution spectra are compared to the observed spectrum in order to get *constraints on the wind physics* or *constraints on the basic parameters* T_{eff}, R_*.

iii) In the test phase it is also worthwhile to check the dynamics by a comparison of the predicted- and the observed mass loss rate; the latter should be

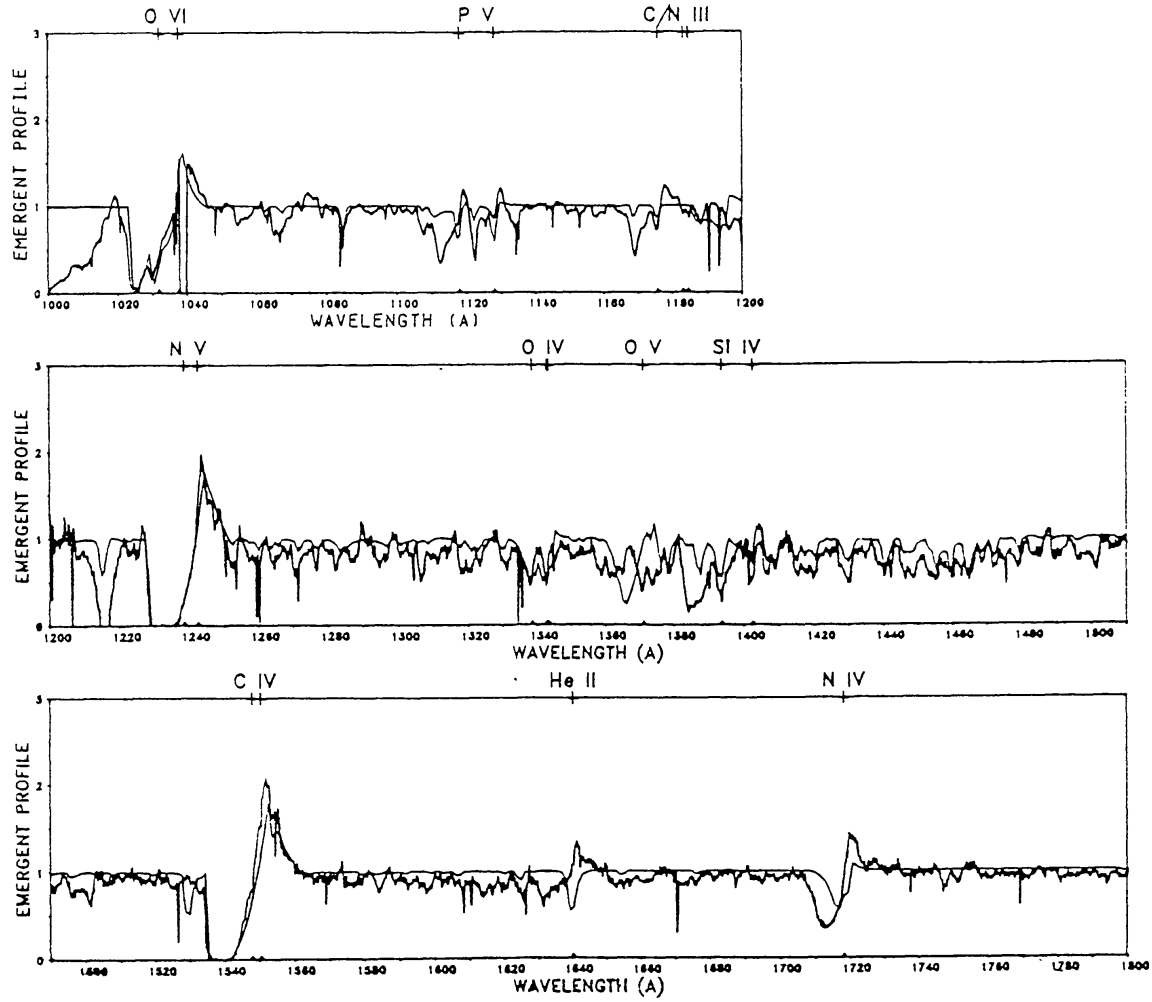

Fig. 4. Calculated and observed UV spectrum for ζ-Pup. The calculated spectrum belongs to model 1.

determined from radio data or H_α.

iv) In the next step the observed- and systhetic spectrum of the final model is compared again for a precise determination of *abundances.*

This procedure provides the diagnostic tool for the determination of complete sets of stellar parameters consisting of *R, L, M, Z* and hence *distance.*

3.1. Analysis of the UV spectrum of ζ-Puppis

In order to verify our method and to show the influence of the crucial points of our treatment metioned in section 2, a series of models will be investigated in the following. For all of these models we adopt a value of $T_{eff} = 42000K, R_*/R_\odot = 19$ and $v_\infty = 2260km/s$ (Groenewegen et al. 1989; Kudritzki et al. 1992 - Paper X). The different assumptions are summarized in Table 1.

3.1.1. Model 1

We start with a spectrum synthesis calculation where the assumptions of paper IX have been adopted - *simplified atomic models*,Kurucz (1979) *LTE-fluxes* are

used to simulate the *EUV line blocking* shortword of the He II groundstate edge, constant temperature in the wind part ($T(r) \approx T_{eff}$) *EUV and X-ray radiation* by shock heated matter *is neglected* and solar abundances are assumed.

TABLE I

Assumptions characterising five different models for ζ-Pup.

model	atomic models	blocking	T_{eff}	shocks	Z	log g	$\dot{M}$ ($10^{-6}\,M_\odot$/yr)
1	simplified	LTE	$T_e = T_{eff}$	no	solar	3.5	3.6
2	*improved*	LTE	$T_e = T_{eff}$	no	solar	3.63	5.1
3		*(N)LTE*	*NLTE*	no	solar	3.63	5.1
4				*yes*	solar	3.63	5.1
5					*spectr.*	3.63	5.1

With these approximations a reasonable value for the mass loss rate is obtained (the actual value obtained from the observed radio flux is in between 3 – 5 $10^{-6}M_\odot$/yr - see discussion in Paper XII) and a surface gravity of log g = 3.5. Although this value coincides with the result from the hydrostatic analysis, it is at least 0.1 dex smaller than the value obtained from the "unified model" (see sect. 1) and thus incorrect. The comparison between the observed and the synthetic spectrum (Fig. 4) shows good agreement for the strong resonance lines of CIV, NV and OVI-the latter indicates that the problem of "superionization" (cf. Lamers and Morton (1976), Cassinelli and Olson (1979), Hamann(1980), Olson and Castor (1981)) can be solved without any other source of ionization (cf. Paper III, Paper IX), but the rest of the spectrum is riddled by striking discrepancies. Among others the FeV lines disagree completely. Hence we have to note that the wind physics is obviously not yet correctly described.

Following the strategy outlined above we will now investigate how far the improved atomic models can influence these mainly negative results.

3.1.2. Model 2

As an example of the new atomic data sets the Grotrian diagram of the most crucial ionization stage in stellar wind calculations-FeV-is displayed in Fig 5. The reasons for the importance of FeV are threefold: 1. FeV shows numerous spectral features in the UV, 2. most of the almost 4000 spectral lines which are available from this atomic model contribute to the photospheric EUV blocking, and 3. up to 50% of the line force in the lower part of the wind-where $\dot{M}$ is fixed-is due to FeV. A change in the opacity-especially the iron opacity-owing to the more accurate and complete atomic data will, therefore, influence not only the spectrum calculation but also the dynamics. As is verified in Fig. 6 far more spectral lines contribute to the line force for model 2. This leads not only to a

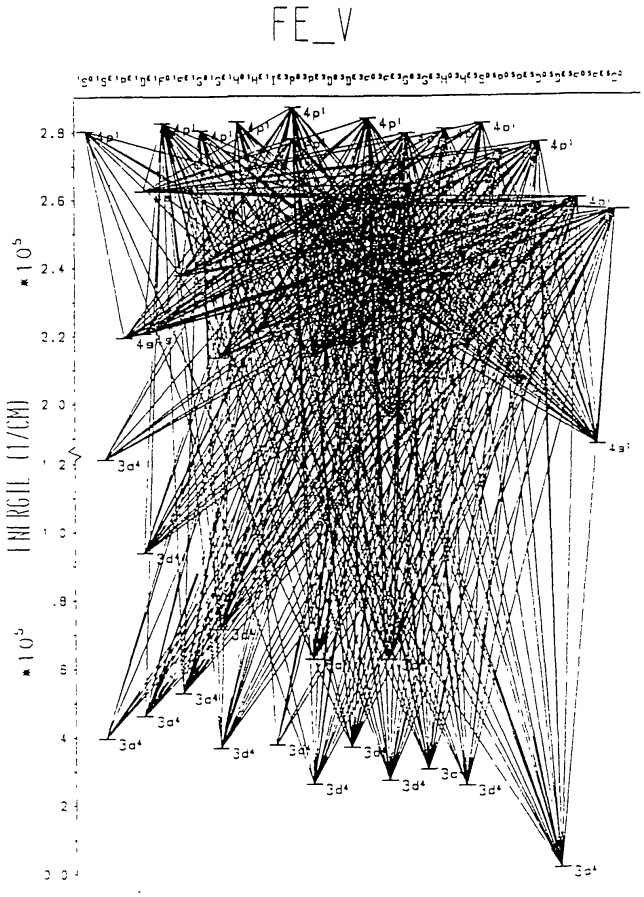

Fig. 5. Grotrian diagram of the atomic model of Fe V.

significantly larger value for the mass-loss rate ($\dot{M}$ = 5.1 $10^{-6}M_{\odot}$/yr),but also to an increased value for the surface gravity (log g = 3.63), which is now exactlythe value obtained by the "unified model".

Concerning the synthetic spectrum of this model the comparison shows some improvements (Fig. 7), e.g. the FeV lines between 1420 to 1480 A are reasonable now, but there are still striking discrepancies. In particular the low ionization stages CIII, NIII, SiIV, and HeII (λ 1640A) disagree completely-instead of characteristic P-Cygni profiles only photospheric components are predicted.

3.1.3. Model 3

Since the ground state edges of these stages (SiIV - 274.4A, NIII - 261.4A, CIII - 258.9A) are located just longward of the HeII edge (227.8A), where photospheric line opacities are significant, the reason for this failure was attributed to insufficient line blocking in this frequency range (Paper VII, Paper IX). However, in Paper XII it turned out that the radiative ionization rates of these species are also strongly influenced by the continuum opacity shortward of the HeII - edge. Too strong an ionization is prevented only if the opacity shortward of 227A is consid-

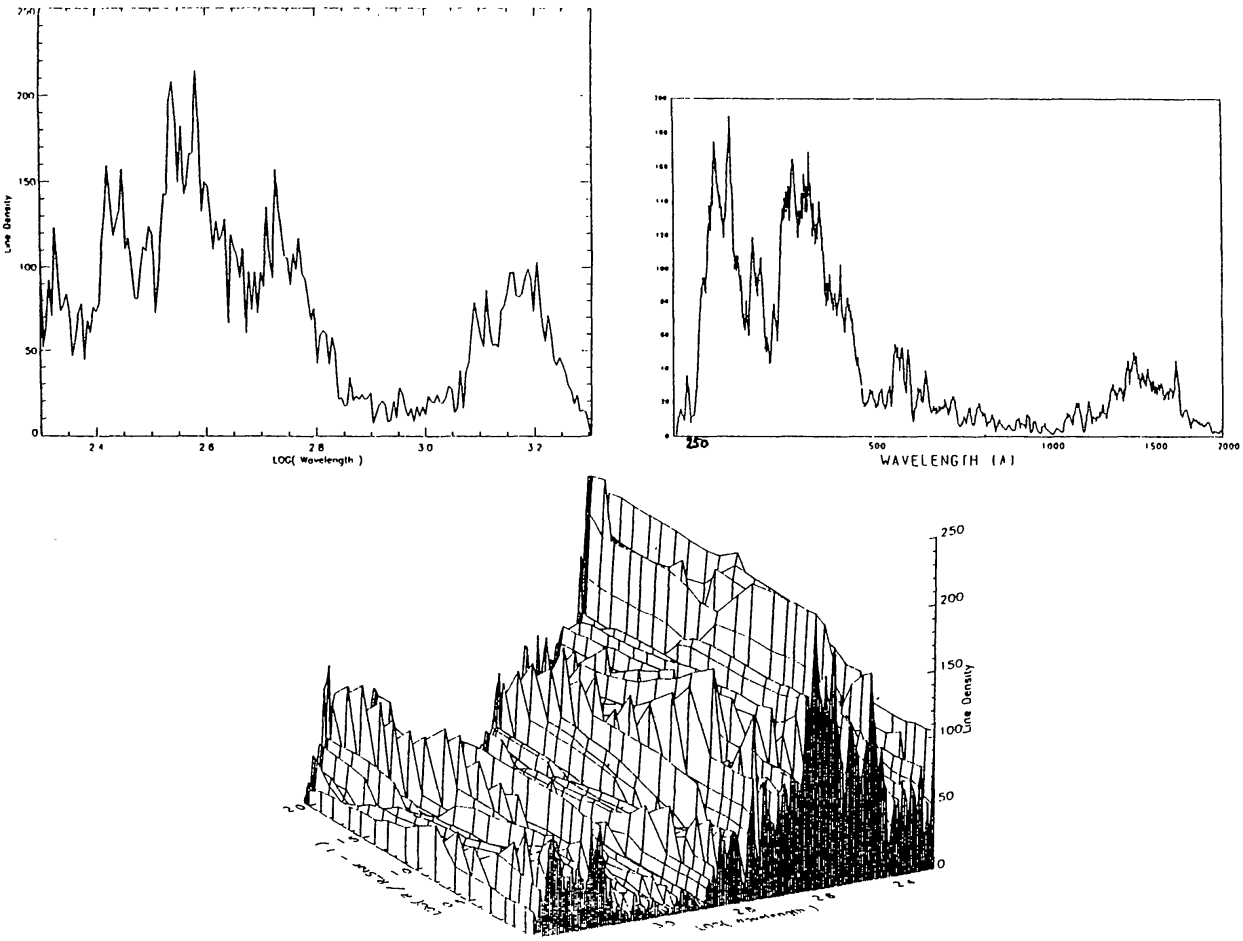

Fig. 6. Projection of line density (number of lines with opacity larger than Thomson-opacity in the maximum Doppler-interval) - upper left, model 2; upper right, model 1 - and line density versus radius and wavelength - below, model 2 - of ζ-Pup.

erably large, so that the radiation field is reduced due to the optical thickness. In Paper XII it was shown that this situation can only be obtained by recombination of HeIII to HeII in the outer wind layer; and this requires not only a *more realistic treatment of photospheric EUV line blocking*,but also a *wind temperature structure* which drops significantly in the outer wind layers. This is the case for *radiative equilibrium* calculations by Gabler (1992).

As the correct treatment of the blocking influence of all metal lines in the entire sub- and supersonically *expanding atmosphere* has not yet been realized (cf. Puls and Pauldrach, 1990), up to now one has had to rely on approximations. So far, Monte Carlo simulations have been performed (Abbott and Lucy (1985), Lucy and Abbott (1992), Schmutz and Schaerer (1992)). However, these calculations suffer from the treatment of line opacities-instead of solving the correct rate equations in NLTE, inadequate gaseous nebula like formula have been used. On the other hand emergent fluxes obtained from conventional hydrostatic NLTE model atmospheres for which the metal line opacity has been included in LTE (Fig. 8) turned out to be not too bad *an approximation*, since our wind models

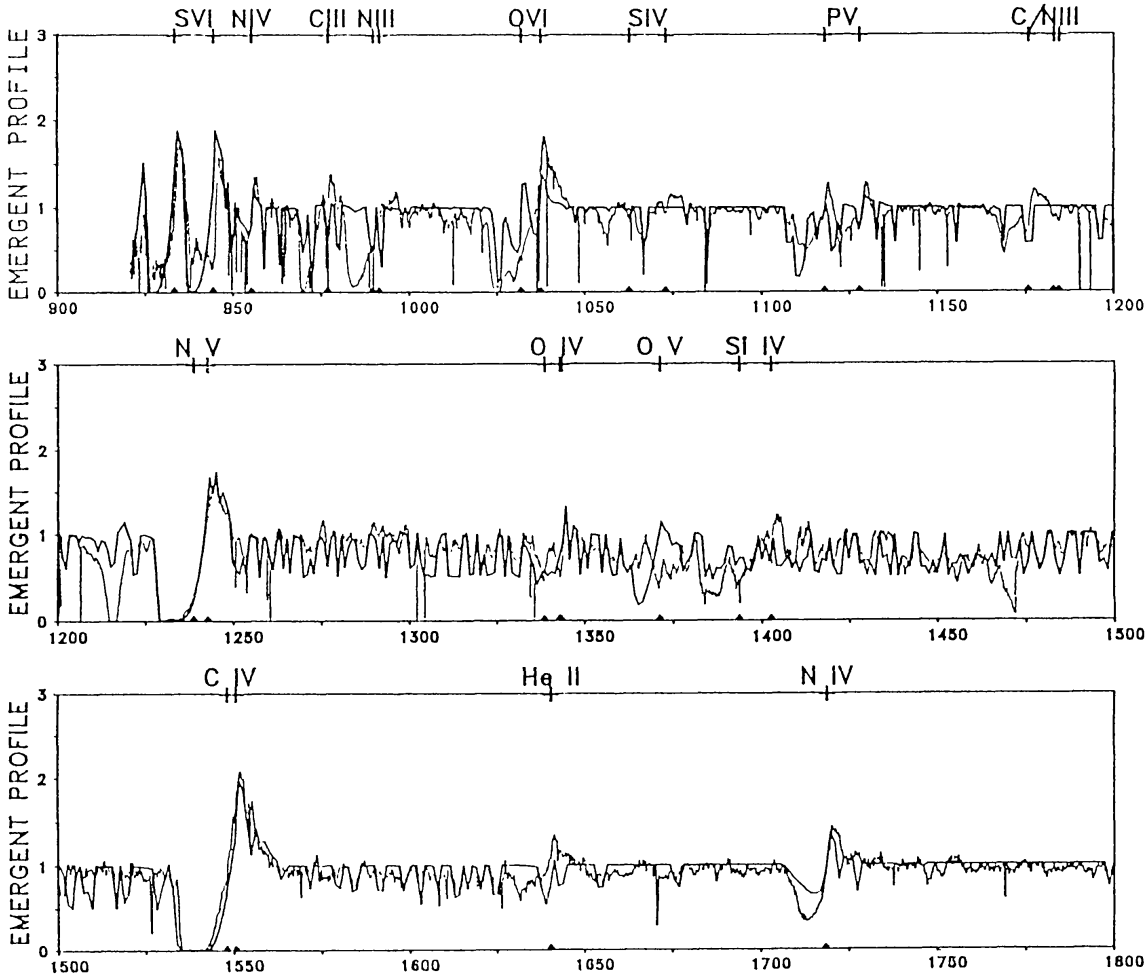

Fig. 7. Calculated and observed UV spectrum for ζ-Pup. The calculated spectrum belongs to model 2. From Paper XII.

showed that the iron like ions dominating the blocking are indeed almost in LTE in the region where the blocking takes place (cf. Paper XII).

Fig. 9 shows the synthetic spectrum of a model calculated with this kind of blocking, reducing the flux significantly shortward of 300A, and with T(r) according to Gabler (1992). This model proved indeed that helium recombined in the outer wind layers. As a consequence of both effects the situation has clearly improved regarding CIII, NIII, SiIV, NIV, OV and HeII 1640, and almost all FeV lines are now represented well. However, these improvements are accompanied by increased deficiencies for high ionization stages like NV and OVI, so that we are again faced with the problem of "superionization". But, as was shown in Paper XII, this problem is solved by accounting for the EUV radiation field of shocks.

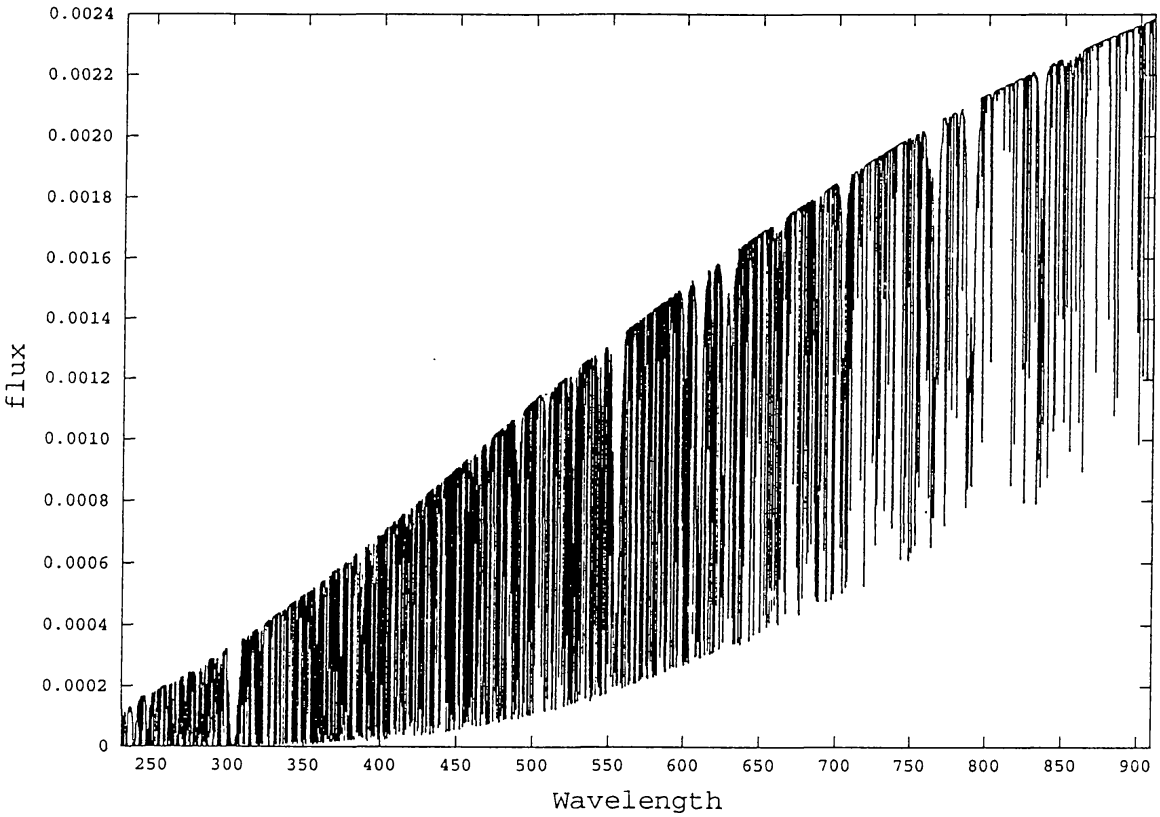

Fig. 8. The emergent flux ($erg/(cm^2 s Hz)$) of a photospheric model of ζ-Pup. in the range 227A- 911A. The influence of blocking due to line opacities if shown. This reduces the radiation field drasically in this frequency regime. From Paper XII.

3.1.4. Model 4

The present scenario for producing the soft X-ray emission of O stars (detected by Seward et al. (1979) and Harnden et al. (1979) where L_x/L_{Bol} is typically 10^{-7} - Chlebowski et al. (1989)) is to assume that they arise from shock instabilities in the stellar wind. This picture was guided by the finding of Lucy and Soloman (1970) that radiation driven winds are inherently unstable. Hence, non-stationary features must show up leading to shocks and the X-rays are explained by radiative losses of the post shock regions (Lucy and White (1980), Lucy (1982)). Although Krolik and Raymond (1985) had already pointed out that shock-heated matter radiates also in the ultraviolet, only the effects of Auger-ionization caused by X-rays were studied to investigate the influence on ionization (Cassinelli and Olson (1979), Olson and Castor 1981), Cassinelli and Swank 1983, Waldron (1980)). This mechanism is, however, probably of secondary importance (cf. Paper IX), whereas enhanced *direct ionization by EUV shock radiation* has important effects (cf. Paper XII).

A consideration of this process requires a theoretical investigation of time dependent radiation-hydrodynamics which describes the creation and developement of shocks (cf. Owocki, Castor and Rybicki (1988), Feldmeier (1993)). From this kind of calculations is turned out that the wind is not inherently unstable as

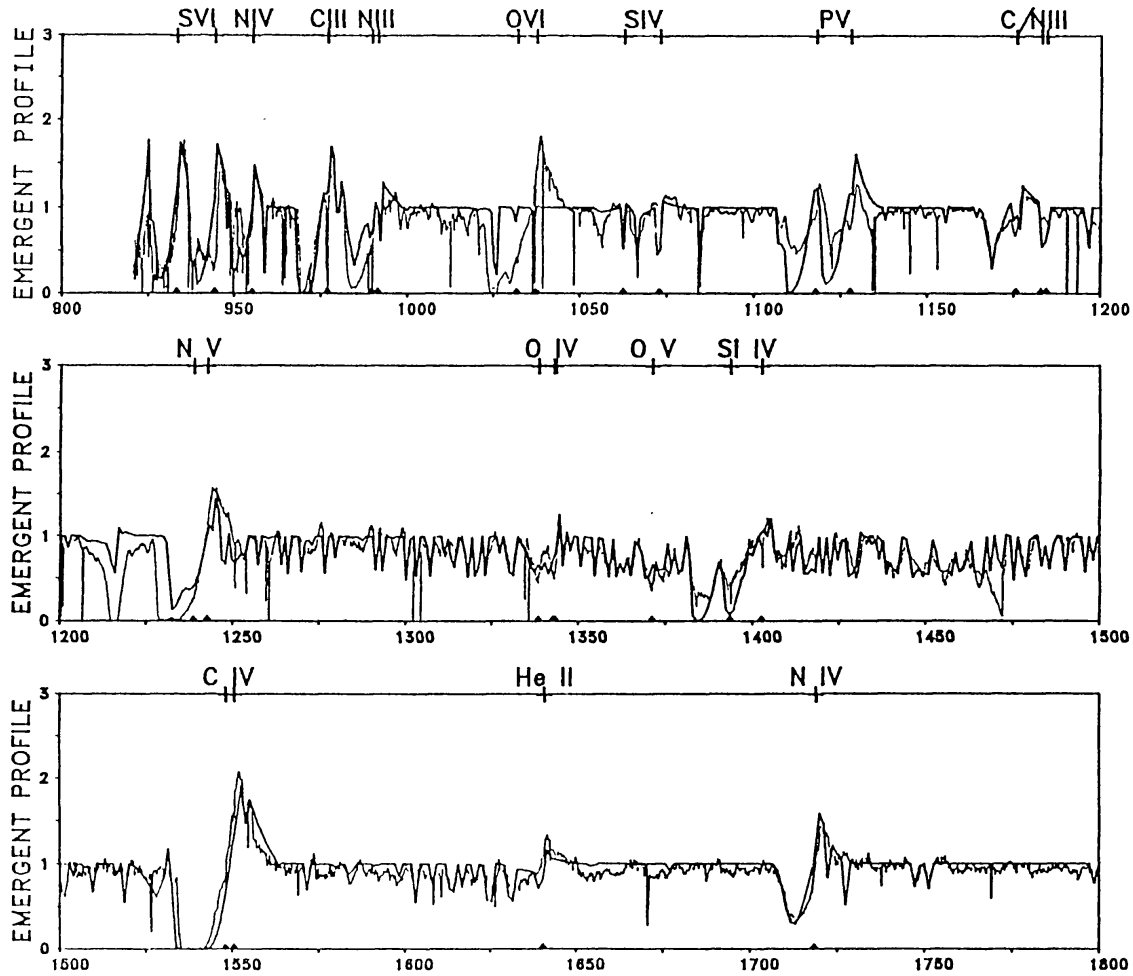

Fig. 9. Calculated and observed UV spectrum for ζ-Pup. The calculated spectrum belongs to model 3. From Paper XII.

was suggested earlier, but is unstable against small perturbations. This is shown in Fig. 10a where the temporal development of $\dot{M}$ is plotted versus radius. After about 10 hours - from model start - the wind settles down to a pronounced periodic response to the perturbations which are described by sound waves with an amplitude of 1% in density and a period of 5000s. Although the spatial variation of the velocity seems to be in contrast to the stationary picture (Fig. 10b), the gross wind properties like the time averaged velocity structure (over 1 hour) and the mass distribution (Fig. 10c) turn out to be in quite good agreement with those of the stationary models. Moreover, since the shock distance is much larger than the shock cooling length in the accelerating port of the wind, the picture of a stationary "cool wind" with embedded randomly distributed shocks is approporiate. Fig. 10c also shows that there is only a small amount of high velocity material (the spikes) which gives a filling factor not much larger than $f^{sh} \sim 10^{-2}$, and from the height of the spikes jump velocities $u^{sh} = 300 - 500$km/s and, hence, immediate post shock temperatures of $T^{sh} = 1 - 3 \cdot 10^6$K are deduced. The reliability of

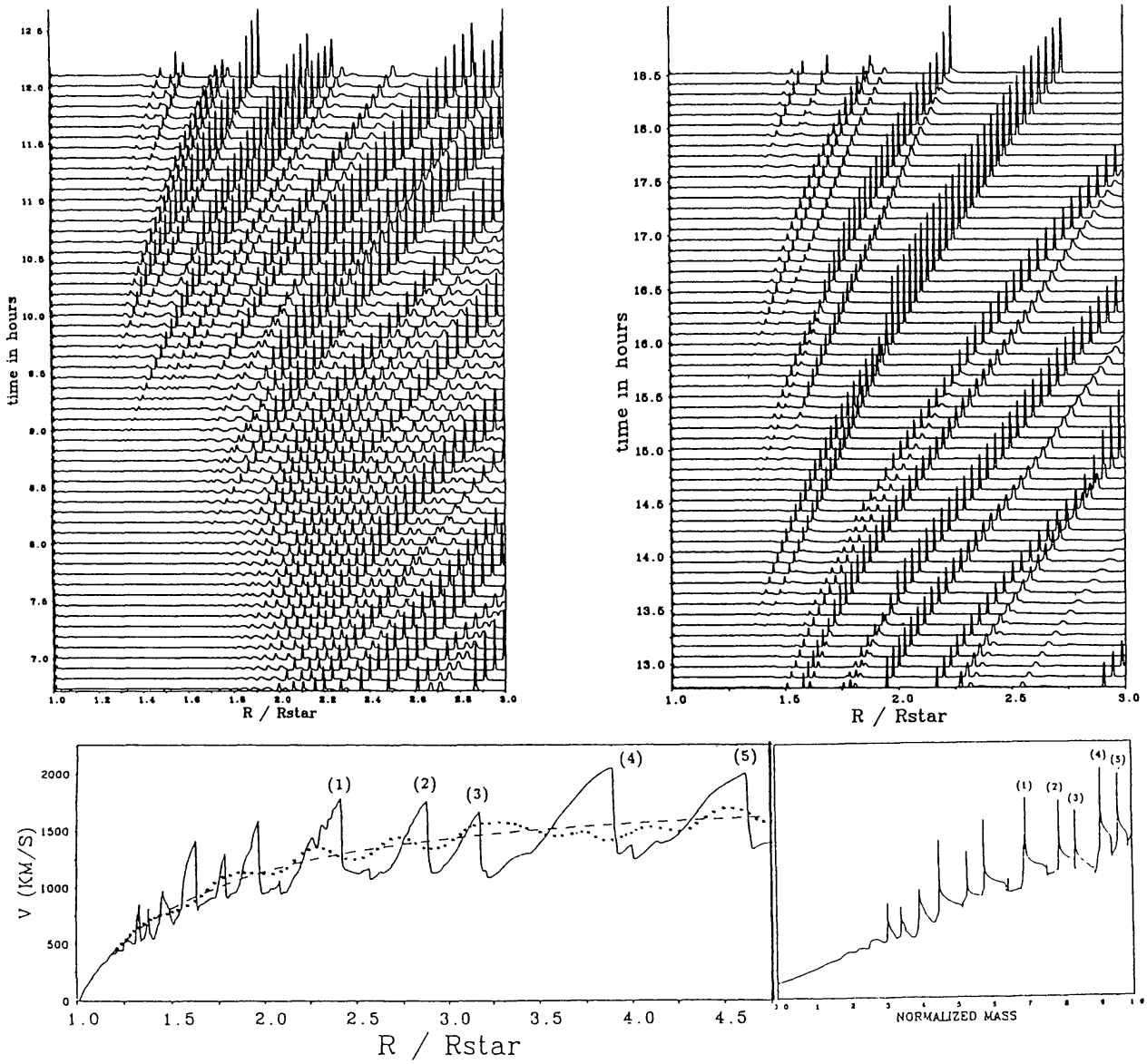

Fig. 10. Temporal development of $\dot{M}$ versus radius (upper part - Fig. 10a). Note the merging shells on the right panel. Velocity at a later time step plotted versus radius (lower panel left - Fig. 10b; stationary model - dashed line; time average over 1 hour - dotted line) and normalized mass (lower panel right - Fig. 10c). Pronounced features are indicated by numbers.

these calculations can be demonstrated by a comparison to ROSAT-observations.

On the basis of this picture the radiative transfer has been solved including shock emission - where the volume emission coefficient (Λ_ν) of an X-ray plasma is calculated using the Raymond and Smith (1977) code and T^{sh} and f^{sh} enter as fit parameters -, K shell absorption and absorption by the "cool wind" (cf. Hillier et al., 1993). A detailed modelling of the observed X-ray spectrum of ζ-Puppis revealed that the fitted jump velocities (n^{sh} = 290 – 520km/s) and filling factors ($f^{sh} = 1.8 - 2.1 \cdot 10^{-2}$) agree quite well with the results of the time

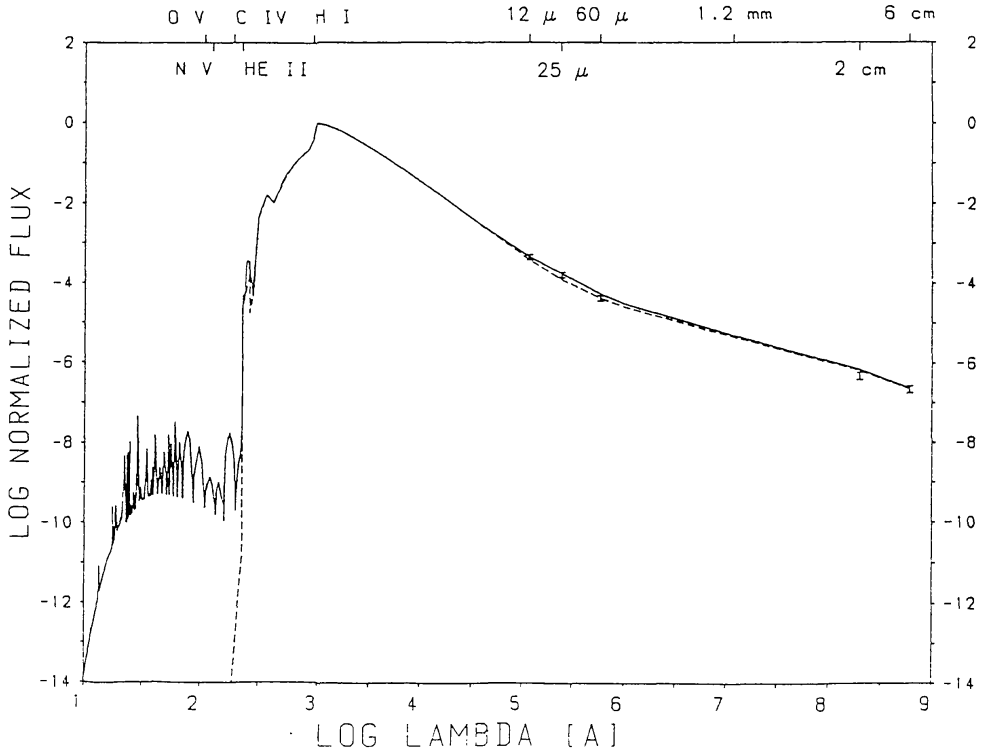

Fig. 11. Energy distribution of two atmospheric models - including shock emission (fully drawn), whithout (dashed) - of ζ-Pup.

dependent calculation, and that the best fit occurs when the cool wind opacity of model 3 is used, i.e. the model where He-recombination takes place. It is further important to note that the jump velocity which fits the energy port below the K-shell edges (u^{sh} = 290km/s) is surprisingly equal to the "turbulence velocity" (v_{turb} = 290±70km/s, Groenewegen et al., 1989). Hence, the primary contribution of shock radiation to the ionization equilibrium by direct ionization is obviously characterized by the shock temperature resulting from $u^{sh}_{max} = v_{turb}$ (cf. Paper XII).

Fig. 11 shows the emergent energy distribution calculated for model 4, where an ad hoc approach for the spatial behaviour of the jump velocities has been adopted and K-shell absorption, Auger-ionization and Λ_ν calculated using the Raymond and Smith code have been included (cf. Paper XII, Hunsinger and Pauldrach, 1994). The influence of shock emission shortward of the HeII edge is significant and reveals the importance of direct ionization due to EUV and soft X-ray photons. This not only affects the high ionization stages - NV, OVI -, but also leads to synthetic lines which reproduce the observations almost perfectly (cf. Fig. 12).

3.1.5. Model 5

At this step we regard the wind physics as correctly described, and the stellar parameters as determined and verified. Hence, the stellar mass $M/M_\odot$ = 55.6

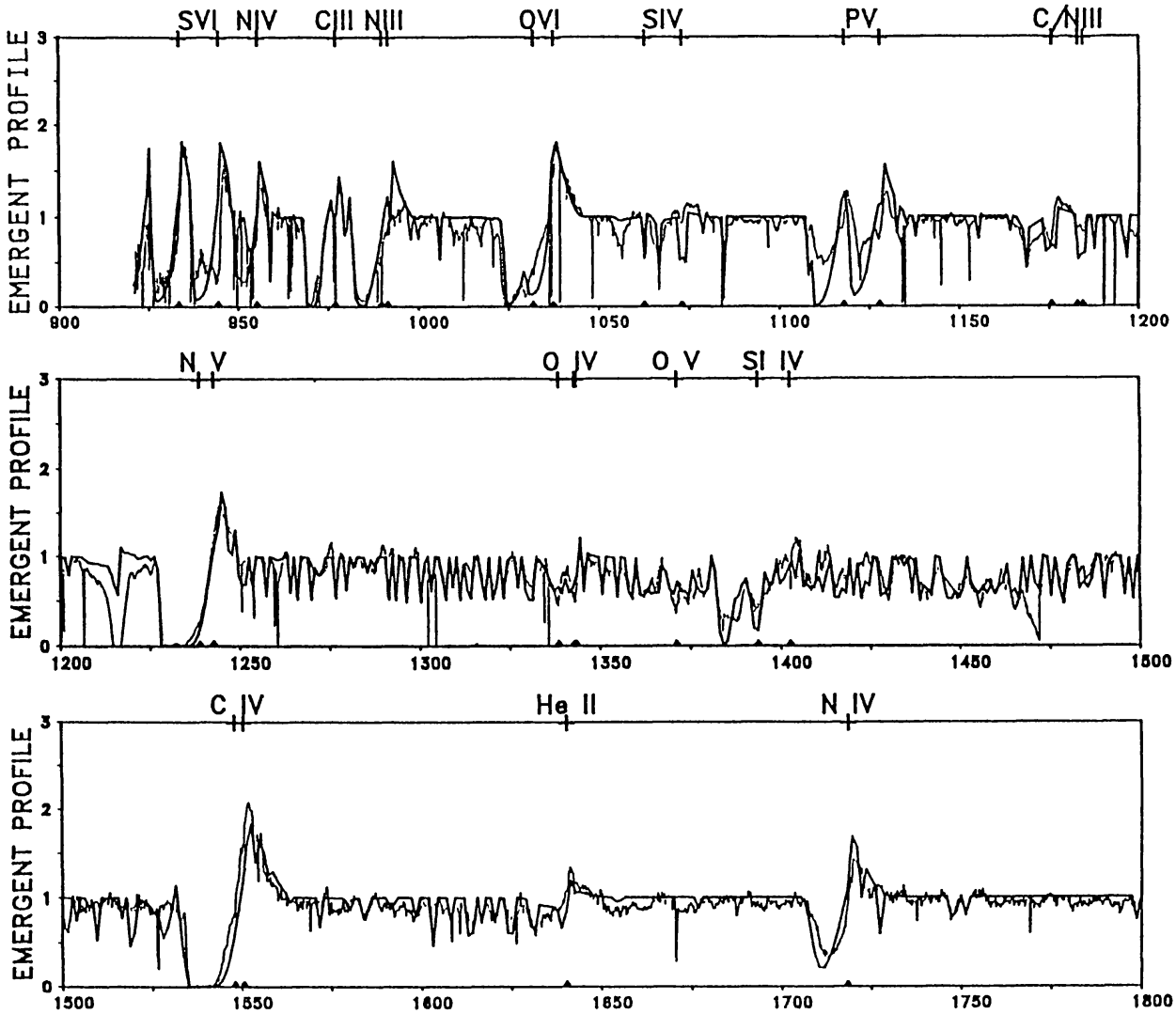

Fig. 12. Calculated and observed UV spectrum for ζ-Pup. The calculated spectrum belongs to model 5.From Paper XII.

obtained from the derived value of the surface gravity can be compared to the mass obtained from stellar evolution theory-$M/M_\odot$ = 68.5 (Maeder, 1990). A difference of only 20% in this case does not support the "mass discrepancy problem" (cf. Groenewegen et al. (1989), Herrero et al. (1992)). The remaining item is the *determination of abundances*. Here we have to consider that ζ-Pup. must be regarded as an evolved object-photospheric analyses showed an enhanced He-abundance (cf. Kudritzki et al. (1983), Voels et al. (1989)). This is supported by the fact that the CIII resonance line of model 3 is too strong and the NIII resonance line is too weak (cf. Fig. 9 - note that both lines are physically affected in the same way). We have, therefore, calculated a model 5 where the CIII resonance line was fitted-yielding $\epsilon_C = 0.35\epsilon_{C,\odot}$ ($\epsilon_{C,\odot}$ is the solar number fraction)-and consistent predictions from evolutionary tracks have been taken for the other elements $-\epsilon_N = 8.0\epsilon_{N,\odot}$, $\epsilon_O = 0.75\epsilon_{O,\odot}$, $n_{He}/n_H = 0.12$ (Maeder, 1990). As is shown in Fig. 12, the observed spectrum is fitted quite well apart from minor differences (a completely independent fit resulted in $\epsilon_N = 4.0\epsilon_{N,\odot}$, $\epsilon_O = 1.0\epsilon_{O,\odot}, \epsilon_P = 0.6\epsilon_{P,\odot}$, $n_{He}/n_H = 0.1 - 0.2$). Therefore, we conclude that

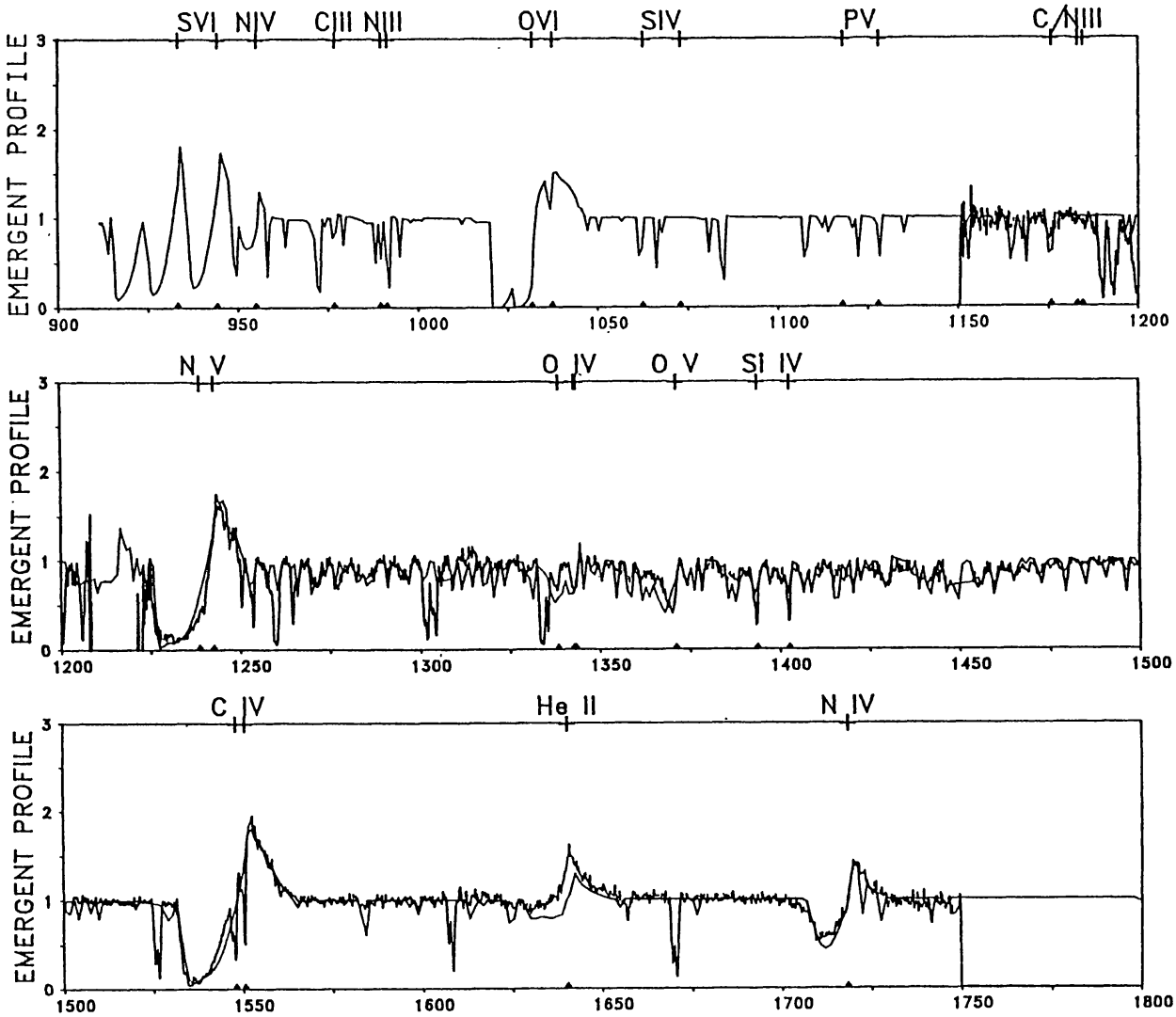

Fig. 13. Calculated and observed (HST high resolution) spectra for Melnick 42. Note that the stellar parameters have been determined using only the tools of UV diagnostics.

our spectrum synthesis technique does already allow the determination of abundances, especially the Fe-abundance can be derived with high precision due to its strong influence on the dynamics which in turn changes the synthetic spectrum considerably.

3.2. Analysis of the UV spectrum of Melnick 42

The UV analysis carried out in Paper XII by incorporating all the improvements discussed above led to the conclusion that the effective temperature (T_{eff} = 50500K) and the surface gravity (log g = 3.8) deduced from the observed terminal velocity (v_∞ = 3000km/s) are much higher than those values derived by Heap et al. (1991) who used hydrostatic atmosphere models ($T_{eff}^{hyd.}$ = 42500K, log $g^{hyd.}$ = 3.5). This conclusion relies on two aspects. 1. The synthetic UV spectrum calculated on the basis of the parameters from Heap et al. showed serious descrepancies compared to the HST observations. 2. A quite reasonable fit of the whole UV spectrum was achieved by a calculation based on a grid of self-consistent mod-

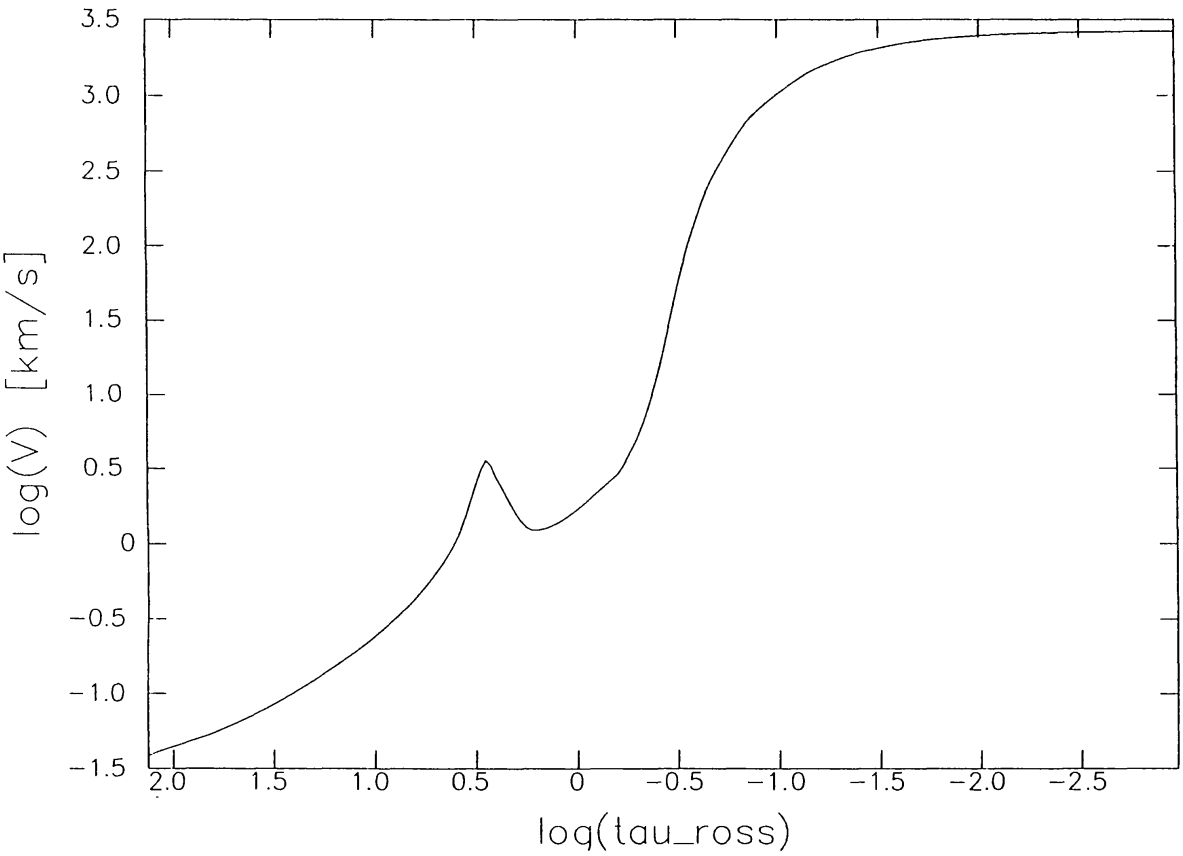

Fig. 14. Velocity versus the Rosseland-optical depth. The influence of the continuous acceleration in the photospherical region is clearly displayed.

els for Melnick 42 (cf. Fig. 13), where $T_{\rm eff}$ was obtained from a comparison of the FeV/IV lines, and the SiIV and CIII line. Furthermore, a much higher mass ($150.4 M_\odot$), luminosity ($\log L/L_\odot = 6.6$) and mass-loss rate ($\dot{M} = 27. \cdot 10^{-6} M_\odot/yr$) were derived consistently, and abundances a factor of four smaller than solar were obtained. Moreover, an extrapolation of Maeder's (1990) evolutionary tracks showed that the corresponding mass of $155 M_\odot$ agrees well with our value. Hence, MK42 does not show indications of the "mass discrepancy" either.

However, one problem remains: The failure of the photospheric analysis. Although it is well known that photospheric lines might be wind contaminated (cf. sect. 1), the effective temperatures derived from hydrostatic atmosphere models are commonly regarded as correct, since they are mainly deduced from the purely hydrostatic HeI λ 4471A line. The presence of this line, with roughly 250mA equivalent width, constrained $T_{\rm eff}$ to a value not higher than 42500K. However, this argument was already weakened in Paper XII, where it was shown that due to the different density structure-compared to hydrostatic calculations-caused by the extremely high $\dot{M}$ of MK42, the EUV blocking influences even deeper regions where the HeI line is formed. It was also shown that the line has a reasonable strength (125mA) when blocking is included in the calculations,

but the line still turned out to be too weak. Hence, we started to investigate a second aspect. This concerns the influence of the continuous acceleration (g_{cont} - cf. sect. 2) due to Thomsom scattering and bound-free and free-free absorption on the photospheric density structure. It turned out from these calculations that the influence of g_{cont} on the velocity and, hence, density structure is considerable at an optical depth of τ_{ROS} 1 – 5 for extremely high values of the mass-loss rate ($\dot{M} > 10 \cdot 10^{-6} M_{\odot}/yr$). In the case of Melnick 42 the velocity increases again to a value of 20% of the sound velocity at τ_{ROS} 3 (cf. Fig. 14). Therefore, an optical depth larger than 10 is required to match the approximation of hydrostatic equilibrium. As the He I line is formed at much smaller depths its spectral shape and, hence, its equivalent width is certainly influenced by this effect; calculations allowing a quantitative investigation of this finding will be forthcoming soon (we note here that the dynamics were only slightly affected by g_{cont} - less than 10% - in the considered range of $\dot{M}$; we note further that the effect decreased considerably if the contribution of the metals was neglected for g_{cont}).

4. Acknowledgements

We wish to thank our colleagues S.M. Haser, Dr. K. Butler, Dr. M. Lennon, C. Kronberger, Dr. R. Gabler for helpful discussions and Dr. D. Lennon for carefully reading the manuscript. This research was supported by the Deutsche Forschungsgemeinschaft in the "Gerhard Hess Programm" under grant PA 477/1-1.

References

Abbott, D.C.: 1982, *Astrophys. J.* **259**, 282
Abbott, D.C. and Lucy, L.B.: 1985, *Astrophys. J.* **288**, 679
Bieging, J.H., Abbott, D.C., Churchwell, E.B.: 1989, *Astrophys. J.* **340**, 518
Bohannan, B., Abbott, D.C., Voels, S.A., Hummer, D.G.: 1986, *Astrophys. J.* **308**, 728
Cassinelli, J.P., Olson, G.L.: 1979, *Astrophys. J.* **229**, 304
Cassinelli, J.P., Swank, J.H.: 1983, *Astrophys. J.* **271**, 681
Castor, J., Abbott, D.C., Klein, R.: 1975, *Astrophys. J.* **195**, 157
Chlebowski, T., Harnden, F.R.,Jr., Sciortione, S.: 1989, *Ap.J.* **341**, 427
Ebbets, D.C.: 1982, *Astrophys. J.* **suppl. 48**, 399
Eisner, W., Jones. M., Nussbaumer, H.: 1974, *Comput. Phys. Commun.* **8**, 270
Feldmeier, A.: 1993, 'Thesis', *Ludwig-Maximilians-Univ.,Muenchen* ,
Gabler, R., Gabler, A., Kudritzki, R.P., Puls, J., Pauldrach, A.W.A.: 1989, *Astron.Astrophys.* **226**, 162
Gabler, R.: 1992, 'Thesis', *Ludwig-Maximilians-Universitaet, Muenchen* ,
Groenewegen, M. A. T., Lamers, H. J. G. L. M., Pauldrach, A. W. A.: 1989, *Astron. Astrophys.* **221**, 78
Hamann, W.R.: 1980, *Astron. Astrophys.* **84**, 342
Harnden, F.R., Jr., Branduardi, G., Elvis, M., Gorenstein, P., Grindlay, J., Pye, J.P., Rosner, R., Topka, K., and Vaiana, G.S.: 1979, *Astrophys. J. (Letters)* **234**, L51
Heap, S. R., Altner, B., Ebbets, D., Hubeny, I., Hutching, J. S., Kudritzki, R. P., Voels, S. A., Haser, S., Pauldrach, A. W. A., Puls, J., Butler, K.: 1991, *Astrophys. J. Letters* **377**, L29
Henrichs, H.F.: 1986, *Pub. Astron. Soc. Pacific* **98**, 48

Herrero, A., Kudritzki,R.P., Vilches,J.M., Kunze,D., Butler,K., Haser,S.: 1992, *Astron.Astrophys.* **261**, 209
Hillier, D.J., Kudritzki,R.P., Pauldrach,A.W.A., Puls,J., Baade,D., Schmitt,J.M.: 1993, *Astron. Astrophys.* **in press**,
Hummer, D.G., Rybicki, G.B.: 1985, *Astrophys. J.* **293**, 258
Hunsinger, J., Pauldrach, A.W.A.: 1994, *Astron.Astrophys.* **in prep.**,
Krolik, J.,H. Raymond, J.C.: 1985, *Astrophys. J.* **298**, 660
Kudritzki, R.P., Simon, K.P., Hamann, W.R.: 1983, *Astron. Astrophys.* **118**, 245
Kudritzki, R.P., Hummer, D.G.: 1990, *Annual Rev. Astron. Astrophys.* **28**, 303
Kudritzki, R. P., Hummer, D. G., Pauldrach, A. W. A., Puls, J., Najarro , F., Imhoff, J.: 1992, *Astron., Astrophys.* **257**, 655(Paper X)
Kurucz, R.L.: 1979, *Astrophys. J. Suppl.* **40**, 1
Lamers, H.J.G.L.M., Morton, D.C.: 1976, *Astrophys. J. Suppl.* **32**, 715
Lamers, H.J.G.L.M., Gathier, R., and Snow, T.P.: 1982, *Astrophys. J.* **258**, 186
Lucy, L.B., Solomon, P.: 1970, *Astrophys. J.* **159**, 879
Lucy. L.B., White, R.: 1980, *Astrophys. J.* **241**, 300
Lucy, L.B.: 1982, *Astrophys. J.* **255**, 286
Lucy, L.B., Abbott, D.C.: 1992, *Ap. J.* **405**, 738
Maeder, A.: 1990, *Astron. Astrophys. Suppl. Ser.* **84**, 139
Mihalas, D., Hummer, D.G.: 1973, *Astrophys. J.* **179**, 872
Morton, D.C., Underhill, A.B.: 1977, *Ap. J. Suppl.* **33**, 83
Nussbaumer, H., Storey, P.J.: 1978, *Astron.Astrophys.* **64**, 139
Olson, G.L., Castor, J.I.: 1981, *Astrophys. J.* **244**, 179
Owocki, S.P., Castor, J.I., Rybicki, G.B.: 1988, *Astrophys. J.* **335**, 914
Pauldrach, A.W.A., Puls, J., Kudritzki, R.P.: 1986, *Astron. Astrophys.* **164**, 86(Paper I)
Pauldrach, A.W.A.: 1987, *Astron. Astrophys.* **183**, 295 (Paper III)
Pauldrach, A.W.A., Herrero, A.: 1988, *Astron. Astrophys.* **199**, 262
Pauldrach, A. W. A., Kudritzki, R. P., Puls, J., Butler, K.: 1990, *Astron. Astrophys.* **228**, 125-154 (Paper VII)
Pauldrach, A. W. A., Puls, J., Gabler, R., Gabler, A.: 1990, *Boulder-Munich workshop, ed. C.D. Garmany, San Francisco : Astronomical Society of the Pacific Conference Series* **7**, 171 (Paper IX)
Pauldrach, A. W. A., Kudritzki, R.P., Puls, J., Butler, K., Hunsinger,J.: 1993, *Astron. Astrophys.* **in press**, Paper XII
Prinja, R.K., Howarth, I.D.: 1986, *Astrophys. J. Suppl.* **61**, 867
Puls, J.: 1987, *Astron. Astrophys.* **184**, 227 (Paper IV)
Puls, J., Hummer, D.G.: 1988, *Astron. Astrophys.* **191**, 87
Puls, J., Pauldrach, A.W.A.: 1990, *in Astronomical Society of the Pacific Confe rence Series 7, "Boulder Munich Workshop ". ed. C.Garmany* **203**,
Raymond, J.C., Smith, B.W.: 1977, *ApJ. Suppl.* **35**, 419
Raymond, J.C.: 1988, *in 'Hot Thin Plasmas in Astrophysics', ed. R. Pallavicini, Kluwer Academic Publishers* **3**,
Schmutz,W., Schaerer,D.: 1992, *Lecture Notes in Physics* **401**, 409
Sellmaier,F., Puls,J., Kudritzki;R.P., Gabler,R., Gabler,A., Voels,S.: 1993, *Astron. Astrophys.* **273**, 533
Seward, F.D., Forman, W.R., Giacconi, R., Griffiths, R.E., Harnden, F.R., Jones, C., Pye, J.P.: 1979, *Astrophys. J. (Letters)* **234**, L55
Voels, S.A., Bohannan, B., Abbott, D.C., Hummer, D.G.: 1989, *Astrophys. J.* **340**, 1073
Walborn, N.R., Nichols-Bohlin, J., Panek, R.J.: 1985, *"IUE Atlas of O-Type Spectra from 1200 to 1900 Angst. ", NASA Reference Publication* **1155**,
Walborn, N.R., Ebbets,D.C., Parker,J.W., Nichols-Bohlin, J., White,R.I.: 1993, *ApJ. Letters, in press* ,
Waldron,W.L.: 1984, *ApJ.* **282**, 256